Line mixing effects in isotropic Raman spectra of pure N2: A classical trajectory study

Sergey V. Ivanov, Christian Boulet, Oleg G. Buzykin, Franck Thibault

Citation: The Journal of Chemical Physics 141, 184306 (2014);
doi: 10.1063/1.4901084

Line mixing effects in isotropic Raman spectra of pure N_2: a classical trajectory study

Sergey V. Ivanov,[1,a)] Christian Boulet,[2] Oleg G. Buzykin,[3] and Franck Thibault [4]

[1]*Institute on Laser and Information Technologies, Russian Academy of Sciences (ILIT RAS), 2, Pionerskaya Str., 142190 Moscow, Troitsk, Russia*

[2]*Institut des Sciences Moléculaires d'Orsay (ISMO), CNRS (UMR8214) and Université Paris-Sud, Bât. 350, Campus d'Orsay F-91405, France*

[3]*Central Aerohydrodynamic Institute (TsAGI), Zhukovski, Moscow Region 140160, Russia*

[4]*Institut de Physique de Rennes, UMR CNRS 6251, Université de Rennes 1, Campus de Beaulieu, Bât. 11B, F-35042 Rennes, France*

Abstract

Line mixing effects in the Q branch of pure N_2 isotropic Raman scattering are studied at room temperature using a classical trajectory method. It is the first study using an extended modified version of Gordon's classical theory of impact broadening and shift of rovibrational lines. The whole relaxation matrix is calculated using an exact 3D classical trajectory method for binary collisions of rigid N_2 molecules employing the most up-to-date intermolecular potential energy surface (PES). A simple symmetrizing procedure is employed to improve off-diagonal cross-sections to make them obeying exactly the principle of detailed balance. The adequacy of the results is confirmed by the sum rule. The comparison is made with available experimental data as well as with benchmark fully quantum close coupling [F. Thibault, C. Boulet, and Q. Ma, J. Chem. Phys. **140**, 044303 (2014)] and refined semi-classical Robert-Bonamy [C. Boulet, Q. Ma, and F. Thibault, J. Chem. Phys. **140**, 084310 (2014)] results. All calculations (classical, quantum and semi-classical) were made using the same PES. The agreement between classical and quantum relaxation matrices is excellent, opening the way to the analysis of more complex molecular systems.

[a)] Author to whom correspondence should be addressed. Electronic mail : serg.vict.ivanov@gmail.com

I. INTRODUCTION

An accurate knowledge of molecular rovibrational spectral line parameters in different gas media is a crucial point for numerous up-to-date spectroscopic applications, such as diagnostics of combustion processes, remote sensing of the atmosphere, etc.[1] The lineshape parameters are built into spectroscopic models targeted at the solution of the inverse problem, namely, the retrieval of gas temperature, pressure and concentrations from measured spectra. Since the results of the solution of the inverse problem are very sensitive to input information of any kind, the requirements for underlying spectroscopic data are very high; a typical accuracy of better than a few percents is now required for adequate atmospheric retrievals of various species.[2, 3]

To ensure these strict requirements there is a need for theoretical methods capable of providing very accurate results for line parameters. Remember that although the capabilities of modern experimental instruments are strong, they are not infinite. There are many situations where the measurements are difficult, or the interpretation of experimental results in a correct and accurate way is extremely challenging, as in the case of the dense molecular spectra, especially, at high temperatures. In these cases a reliable theoretical model is clearly needed.

Two sources of error are obviously present in line broadening calculations: the first arises from the inaccuracy of the intermolecular potential energy surface (PES) and the second is related to approximations in the theory itself. The most accurate, robust and realistic PESs are *ab initio* ones which are produced from the first principles and do not contain adjustable parameters. The rapid progress of computational resources over the last two decades allowed such PESs to be obtained for many simple molecular pairs. Only *ab initio* PESs (or refined ones on various experimental kinds of data) should be used in broadening calculations if we want to obtain accurate and reliable results.

As for theory, the most accurate are full quantum calculations within the exact close coupling (CC) method[4] or within the coupled states (CS) approximation[5]. It is clear that only full quantum CC/CS calculations using *ab initio* PESs can ensure the required high level of accuracy and provide benchmark results. However, both computational schemes, particularly the CC one, become extremely time-consuming and unfeasible when many rotational states are populated. Therefore, practical applications of these methods are restricted to simple molecular systems (two diatomics or even simpler ones) at not too high values of the rotational quantum number J, mainly at low and room temperatures.

In an attempt to overcome this difficulty, alternative more approximate theories have been developed: semi-classical[6-14] and classical.[15-20]

Semi-classical methods treat the translational motion classically, but the internal motions (vibration and rotation) are modeled within quantum mechanics. A major defect of all these methods is the lack of self-consistency, i.e., the inability to account exactly for interactions of the translational and internal motions of colliding molecules. In all semi-classical methods, the influence of internal motion on the classical path and back-influence are ignored. As a result, some essential features connected with rotation–translation coupling are completely omitted. For example, the formation of metastable collision complexes (Feshbach resonances) is impossible (see Refs. 21, 22 and the references therein). The second kind of semi-classical simplifications are related to the quantum mechanical characterization of rotation (see Refs. 1, 14, 23). It is well known that only in the most rigorous semi-classical formalism of Neilsen and Gordon[8,9] is the scattering matrix for the rotation of the active molecule calculated exactly using a numerical solution of the time-dependent Schrödinger equation. All other semi-classical schemes (namely, peaking approximation,[10, 23] Smith-Giraud-Cooper method,[10] Anderson method,[6, 7] Robert-Bonamy formalism,[11] etc.) are no longer rigorous in this regard because they contain different intrinsic approximations

simplifying an exact quantum description of the rotational motion.[1, 14, 23] Note that the validity of these approximations is hard to estimate in most cases. Such a picture is similar to the hierarchy of purely quantum methods (CC, CS, IOS, etc.): the ease of computations is achieved by spoiling the physics.

At present and for the last three decades, the most widely used semi-classical method in pressure broadening and shift calculations is that of Robert and Bonamy (RB) - the traditional formalism with parabolic trajectories[11] and its modified versions, namely, complex implementation[12] and the variant with "exact" "isotropic trajectories" (see Ref. 14 and references therein). In a recent paper,[13] a new refined RB formalism was proposed which includes line coupling effects, reducing significantly the difference between semi-classical and quantum half-widths obtained from the same *ab initio* PES without any fitting parameters. At the same time, it becomes possible to calculate the off-diagonal elements of the relaxation matrix[24] W.

The classical approach in impact line broadening, shifting and line mixing calculations was first proposed in 1966 by Roy Gordon.[15, 16] Further extensions and explanations are described in Refs. 17-20. The classical approach ensures an exact three-dimensional (3D) self-consistent characterization of rotational and translational molecular motions. This method is simple, visual and computationally efficient. Brought to revival a decade ago (see Refs. 25-27 and references therein) the classical approach, via its application to many atom-diatom and diatom-diatom molecular systems, has acquired a reputation as a very efficient and quite accurate tool which allows line broadening coefficients to be obtained that are in much better agreement with benchmark and/or experimental data than the results of semi-classical formalisms.

Note that the interpretation of dense molecular spectra with overlapped components is a more challenging problem since it requires the knowledge of the whole relaxation matrix

W.[1] When spectral lines overlap (this depends obviously on pressure and the distance between adjacent components), the off-diagonal elements of the W matrix can no longer be neglected since they lead to line mixing effects, i.e., transfer of intensity between the various lines. Such effects are noticeable in the isotropic Raman Q branch of N_2 at pressures higher than 1 atm.[28] In Ref. 29 CC/CS benchmark relaxation matrix elements were obtained for Raman Q lines of autoperturbed N_2 at room temperature starting from the most accurate *ab initio* N_2-N_2 PES.[30] In a subsequent paper[24] the refined semi-classical RB method[13] was applied to reproduce these benchmark data, requiring empirical corrections for the effects of inelasticity in order to obtain a reasonable agreement with the quantum off-diagonal elements of Ref. 29.

In the present paper, Gordon's classical impact theory is applied for the first time to the calculation of the whole relaxation matrix for the same system.

Section II gives a brief summary of R. Gordon's classical impact theory in respect to isotropic Raman Q lines and the details of trajectory calculations including potential energy surface for N_2-N_2 interactions. In Section III the results obtained are discussed and compared with quantum CC/CS and refined semi-classical RB calculations as well as with experimental values. Section IV summarizes the conclusions.

II. THEORY

A. Basics of classical impact theory

Within the binary collision and impact approximation the spectral density can be written as[20]

$$F(\omega) = \frac{1}{\pi} \mathrm{Im} \left[\frac{\vec{d} \cdot p \cdot \vec{d}}{\omega \cdot I - \omega_0 - iW} \right], \qquad (1)$$

where ω is the angular frequency of radiation, I is a unit diagonal matrix, ω_0 is a diagonal matrix of spectral line positions (frequencies) at low pressures (in the case of single branch its dimension is equal to the number of populated rotational states), $\vec{d}$ is a vector of transition amplitudes (dipole moments or polarizabilities) which determines the intensity of each spectral line, p is a diagonal matrix of the Boltzmann factors for the initial state of each line: the relative population of the lower state of the transition "i" at temperature T is $p_i = \frac{g_{Ii}(2J_i+1)}{Z}\exp\left(-\frac{E_i''}{k_B T}\right)$, where g_{Ii} is nuclear spin statistical weight, J_i is rotational quantum number, Z is partition function, E_i'' is lower state energy, k_B is the Boltzmann constant. The central object in Eq. (1) is the relaxation matrix W. When rotational phase shifts are neglected (as in the case of a hypothetical purely rotational Raman isotropic Q branch), each diagonal element of the W matrix represents the rate at which molecules leave the state associated with that line; the off-diagonal elements W_{fi} are equal to minus the rate at which molecules radiating in line "i" leave that line to join line "f". It is convenient to express the relaxation matrix in terms of the collision cross-sections matrix σ (often called the pressure broadening cross-section matrix):

$$W = n\bar{v}\sigma, \qquad \sigma = \bar{v}^{-1} < v(1-S) >_{b,v,O} \tag{2}$$

Here n is the number density of buffer molecules, $\bar{v} = \sqrt{\frac{8k_B T}{\pi\mu}}$ is the mean relative speed of colliding pair (μ being the reduced mass). The averaging <…> is made over all kinds of collisions, i.e., over initial conditions: impact parameter b, relative speed v, orientations O of molecules and their angular momenta. In doing this average it is assumed that successive collisions are uncorrelated. The classical formulas for the elements of the $(1 - S)$ matrix are presented, for example, in Ref. 16 for different kinds of molecular spectra.

The simplest case of pressure broadening cross-section matrix elements is realized for the Q lines of isotropic Raman scattering also neglecting vibrational phase shift (see Eq. (23) of Ref. 16):

$$\sigma_{fi} = \bar{v}^{-1} < v(\delta_{fi} - P_{fi}) >_{b,v,O} \tag{3}$$

Here δ_{fi} is the Kronecker symbol, P_{fi} is the probability that a collision transfers the rotation frequency of molecule from line "i" (before collision) to line "f" (after collision). That collisions may be interpreted as transferring intensity between the lines of the spectrum is the central point of Gordon's classical broadening theory.[16]

The transition probability P_{fi} can be determined from classical dynamical calculations using the correspondence principle. Its simplest variant rounds off the classical angular momentum to the nearest multiple of Planck's constant $\hbar$. If this is done for initial (before collision) and final (after collision) angular momenta, then $P_{fi} = 1$ for the pair of lines $i \rightarrow f$ with the proper values J_i and J_f of initial and final lower state rotational quantum numbers. All other P_{fi} in Eq. (3) are set equal to zero.

At low pressures when lines are well separated only the diagonal elements of the relaxation matrix are large enough to contribute to the spectrum. In this case the spectrum $F(\omega)$ in Eq. (1) reduces to a sum of isolated Lorentzians whose widths and shifts are directly proportional to the pressure. As the pressure increases, the broadened individual lines begin to overlap, the off-diagonal elements create interferences between the lines (or "line mixing") and cause collisional narrowing effects. Note that for the fundamental Raman Q branch of N_2, at pressures greater than ~1 atm, the off-diagonal elements in W cannot be neglected.[27]

The W matrix computed in the above way may not strictly obey the detailed balance which is the fundamental principle of statistical physics of equilibrium gases. This is partly

due to the limited number of collisions, in particular for elements of the matrix far off the diagonal (large $|J - J'|$ values). Our special calculations made using different numbers of collisions have confirmed this suggestion. Also, there are other factors influencing detailed balance, e.g., the correspondence principle. The procedure for determining the transition probability described above is too crude and may be the cause of detailed balance violation. Obviously, the elaboration of a more sophisticated algorithm for P_{fi} is a subject for future work (some simple suggestion for P_{fi} improvement was proposed as far back as in Ref. 20).

However, the principle of detailed balance can be artificially restored *a posteriori* to improve the cross-sections in the regions where there are fewer trajectories. If detailed balance holds, the number of molecules going from the line "*i*" to line "*f*" per unit time should be equal to those going in opposite direction. So,

$$W_{fi} p_i = W_{if} p_f , \qquad \sigma_{fi} p_i = \sigma_{if} p_f \tag{4}$$

In Ref. 20 a simple symmetrizing procedure was proposed to redefine the elements of the cross-section matrix σ to satisfy the detailed balance:

$$\sigma_{fi}^{DB} = (N_i + N_f)^{-1}[N_i \sigma_{fi} + N_f (p_f / p_i)\sigma_{if}] \tag{5}$$

Here N_i and N_f are the numbers of trajectories from which σ_{fi} and σ_{if} are computed respectively. Note that this procedure modifies only off-diagonal elements leaving the diagonal ones unchanged.

B. Details of classical trajectory calculations

In all our dynamical calculations we employed the N_2-N_2 *ab initio* PES[30] determined by the symmetry adapted perturbation theory (SAPT) which is the most accurate to date and which was also used in our recent works.[13, 24, 26, 29, 31] The molecules were treated as rigid

rotors, so the PES is four-dimensional. It has been developed over bispherical harmonics and the expansion retained 30 angular functions.

Classical calculations were performed using Gordon's impact theory (see above, Section A) at the room temperature T = 298 K. We only present here matrices corresponding to even J and J' values (ortho-N_2) ranging from 0 to $J_{max} = J'_{max} = 28$.

Dynamical calculations of $^{14}N_2 - {}^{14}N_2$ collisions were made using the exact classical three-dimensional (C3D) equations of motion. The collision of two rigid linear molecules in this picture is described by 17 first-order Hamilton differential equations in body-fixed coordinates (their explicit form can be found in the Appendix of Ref. 25). For the sake of comparison with semi-classical results, we also used in our calculations a simplified C3Diso model of "isotropic trajectories" which employs a classical path driven only by the isotropic term ($L_1 = L_2 = L = 0$) in the PES expansion over bispherical harmonics.[26, 30] This C3Diso model is described by 15 first-order Hamilton differential equations.

Classical trajectory equations, both exact C3D and simplified C3Diso, were integrated numerically by the standard IMSL routine for the implicit BDF Gear method.[32] All the calculations were conducted using double precision with a typical tolerance parameter of 10^{-8} and a variable integration step in constant time-grid intervals $\Delta t = 0.05 \cdot 10^{-13}$ s.

The length of the $^{14}N_2$ molecules was set equal to 1.1 Å and the rotational constant B = 1.9896 cm^{-1}. Spin statistical weights of perturbing N_2 molecules at equilibrium were taken into account in the usual way and set to 2/3 for ortho-N_2 and 1/3 for para-N_2. The initial intermolecular distance was set large enough (R_{max} = 15 Å) to exclude starting interaction between the molecules. Other collision parameters were selected via a Monte Carlo procedure. The Maxwell-Boltzmann distribution was used to sample relative speeds at temperature T. Uniform sampling was applied to select initial orientations of angular momenta and molecular axes of both N_2 molecules in 3D space.

The initial rotation frequency of the active N_2 molecule was determined via its discrete rotational quantum number J by the rigid rotor formula $\omega_0 = \frac{2B}{\hbar}(J+1/2)$ (B and $\hbar$ being rotational constant and Planck's constant, respectively) often called a Langer prescription.[33, 34] It is much closer to reality for J = 0, 1 than the usual quantum-mechanical formula $\omega_0 = \frac{2B}{\hbar}\sqrt{J(J+1)}$; for other J values the difference between these two formulae is negligible. Also, in the present calculations a very efficient algorithm[34] for impact parameter sampling (twice as fast as the traditional uniform b^2 sampling) was applied. The initial rotation frequency of the perturbing N_2 molecule was selected using a Monte Carlo method assuming discrete Boltzmann distribution.

The collision parameters were selected as follows: impact parameter (0–12) Å; relative speed (0.01–3)v_p . Here $v_p = \sqrt{\frac{2k_BT}{\mu}}$ is the most probable relative speed of the colliding pair (μ = 14 u being the reduced mass of $^{14}N_2$ – $^{14}N_2$ system). In our calculations the statistical errors, i.e., root-mean-square (RMS) errors of Monte Carlo averaging, for diagonal elements of relaxation matrix (half-widths) were generally kept at less than 1%. This took ~ 86,000 trajectories for C3D method per each J value and ~ 111,000 trajectories for C3Diso method in the same conditions.

III. RESULTS AND DISCUSSION

The results of these calculations are presented in Tables I - IV and in Fig. 1 - 3. Note once more that all classical results were calculated using Maxwell-Boltzmann velocity averaging (RMS Monte Carlo error was < 1% for diagonal elements of W matrix in all cases).

In Table I the comparison is made between classical (C3D and C3Diso), fully quantum CC/CS results and the experimental data of Sitz and Farrow.[35] This table is the extension of

Table III of Ref. 29 and gives very valuable additional information. We give the results for both C3D and C3Diso for two kinds of calculations: (1) applying detailed balance (DB) principle via the symmetrizing procedure of Gordon and McGinnis (σ^{DB}, Eq. (5), upper value in each cell) and (2) without imposing detailed balance (σ, raw trajectory results, lower value in each cell). The N_2 rotational relaxation rate constants (in $\mu s^{-1}Torr^{-1}$) presented in Table I correspond (about to truncation errors) to those in the full *W* matrix (see Table II), via the factor of 1000/(-247.85) (see Ref. 35).

The results of exact classical C3D calculations are in very good agreement with both quantum CC/CS results and experimental data. Also, one may observe that C3D results obtained with the detailed balance symmetrizing procedure of Eq. (5) (case (1) in the following) are noticeably better than without it. The results of case (1) are consistently somewhat higher than CC/CS results, the absolute value of the relative distance being less than 28% (mean 8%). In case (2) (without detailed balance) the C3D results noticeably oscillate around the CC/CS values. The absolute value of the relative difference in this case is less than 31% (mean 14%).

For the C3Diso values the situation is quite different than those for the exact C3D. In both cases the C3Diso results strongly oscillate about the CC/CS values. The corresponding errors are as follows: in case (1) < 100% (mean 20%); in case (2) < 106% (mean 32%). All these results are illustrated in Fig. 1.

Table II contains complete information for all rotational transitions up to $J = 14$. This table is the extension of Table IV of Ref. 35. Each cell of this table contains five positions corresponding to the results obtained using different methods: 1-st - quantum CC/CS; 2-nd - exact C3D with imposed detailed balance (DB); 3-rd - exact C3D but no imposed DB; 4-th - C3Diso with imposed DB; 5-th - C3Diso no imposed DB. Diagonal elements (half-widths) were reported and discussed in Ref. 26. For rotational transitions not included in Table I the

accuracy estimates for the methods used are nearly the same as for Table I and the conclusion is that the C3Diso method works badly, especially, for large $|J - J'|$ values. Note that a similar result was obtained from the semi-classical approach of Ref. 24, corroborating the necessity of taking into account the translational-rotational coupling in such cases of high inelasticity.

It is worth asking the following question: to what degree do our raw, unprocessed data from the classical calculations obey detailed balancing ? Table III displays relative errors (in % as compared to symmetrized by Eq. (5) values) in the detailed balance in raw C3D (upper value) and C3Diso (lower value) calculations of the relaxation matrix W. One can see that raw C3D calculations respect reasonably well detailed balancing. In other words, the empirical Gordon-McGinnis symmetrization procedure seems to be of slight influence in this case (except for the transitions from J = 2-8 to J' = 0). As for raw C3Diso calculations, they almost always respect more poorly the detailed balancing requirement. We can propose some explanations of these interesting facts. First, if we apply the Maxwell distribution over initial speeds of molecules at temperature T for averaging and if the dynamics of rotational exchange in collisions is correct, then we will reproduce the Boltzmann distribution over rotational J levels at temperature T. In other words, direct and inverse cross sections for rotational transitions in collisions will obey detailed balance. Calculations indeed showed that this is the case for C3D for most transitions, but not for the C3Diso case. So, we may assert that the degree of detailed balancing in raw trajectory calculations (in Maxwell velocity equilibrium) is a measure of the adequacy of the description of rotational exchange in collisions.

There exists also a useful and significant property called the sum rule, namely, $\sum_{J'=0}^{J'_{max}} W_{J'J} = 0$ which can be also rewritten as $W_{JJ} = -\sum_{\substack{J'=0 \\ J' \neq J}}^{J'_{max}} W_{J'J}$. As shown in Appendix A, Gordon's formalism (without the empirical symmetrization procedure) verifies exactly that

relation. Table IV displays how the sum rule is satisfied in different classical calculations. One can see that for both C3D and C3Diso "unprocessed" data the sum rule is well-respected, in agreement with theory. Note that the non-zero but very small departure from the sum rule in our trajectory calculations simply reflects the truncation of the sum over J' to a too low value J'_{max}. In other words, inelastic collisions with $J' > J'_{max} = 28$ were simply ignored. This is confirmed by the fact that the error increases with increasing J (see Table IV).

When the detailed balance symmetrization procedure is applied then the fulfillment of the sum rule is much worse, especially in the C3Diso case. First, note that in the C3D case, imposing the empirical Gordon and McGinnis symmetrization procedure leads only to a slight deterioration of the sum rule. In contrast, in the C3Diso case, the deviation from the detailed balance in raw C3Diso data is very strong, much stronger than in C3D calculations. So, it is not surprising that artificially imposing detailed balance for final data spoils the sum rule since detailed balancing is not respected in the raw data. If both the sum rule and the detailed balance are needed with a greater accuracy, new more sophisticated classical trajectory codes should be written. It is the subject for future work.

Summing up, one may assert that: 1) when detailed balance is not imposed, both C3D and C3Diso verify the sum rule, in agreement with theory; 2) in the C3D case, the sum rule remains within the limit of experimental uncertainty when detailed balance is imposed; 3) C3Diso results are somewhat worse than exact C3D, especially, when detailed balance is not imposed; 4) the sum rule is generally violated if we impose detailed balance in C3Diso calculations. This result is similar to that obtained in the semi-classical formalism of Ref. 24 where it was not possible to obtain relaxation matrix elements verifying at the same time detailed balance and the sum rule.

Let us now make a more detailed comparison with semi-classical results obtained using the recently refined Robert-Bonamy formalism.[13] Diagonal elements (half-widths) as a

function of rotational quantum number J are presented in Fig. 2. One can see that the classical results are much closer to the quantum CC/CS values than the semi-classical results. It is curious that the C3Diso results look better than the C3D ones, however, this fact is deceiving and, undoubtedly, does not reflect real physics. Note also that both classical C3Diso and semi-classical Robert-Bonamy calculations are obtained using the trajectories driven by the same isotropic part of the PES. However, their results differ significantly.

Selected off-diagonal elements as a function of J are presented in Fig. 3. As for diagonal elements, the results of classical calculations are in good agreement with quantum values. At the same time, the refined RB method disagrees strongly, particularly for upward transitions ($J' > J$) corresponding to the greater inelasticity which required empirical procedures to introduce in some simple way the exchange of energy between translation and rotation. While going in the right direction for most upward transitions (see Fig. 3, curve 7), these procedures were too crude to provide at the same time via the sum rule, line widths in good agreement with the quantum benchmark data, in contrast to the present classical approach. Further work is clearly needed but there is no doubt that classical calculations will be of great help in understanding the various remaining limits of semi-classical models.

IV. CONCLUSION

Here, for the first time, we have applied Gordon's classical impact theory in order to calculate the full relaxation matrix for Q lines of isotropic Raman scattering in autoperturbed N_2 without any simplification. Alternative computational methods are needed due to the complexity of full quantum CC/CS calculations. For example, even at room temperature the numerical problems that arise are associated with the convergence of the quantum calculations of N_2-N_2 relaxation matrix.[29] Classical calculations are free from the troubles of such sort.

This study demonstrates that the undeservedly forgotten classical impact theory of Roy G. Gordon is capable of remarkable accuracy and has great potential for the simulation of line interference effects in molecular spectra. We are sure that classical impact theory should be developed further in different aspects, in particular: 1) further improvement in accuracy; 2) straightforward application to Raman anisotropic, dipolar and multiplet spectra of linear molecules (the formalism was already developed by R.G. Gordon in Refs. 16, 17); 3) extension of theory and application to other types of molecules (symmetric and asymmetric tops; fortunately, the formulae of Ref. 17 can be directly applied to symmetric tops).

ACKNOWLEDGMENTS

The authors thank Dr. Kevin Dunseath (Rennes) for his careful reading of the paper.

APPENDIX A: THE SUM RULE WITHIN CLASSICAL GORDON'S FORMALISM

1. Consider a diatomic molecule in a rotational level J and all inelastic transitions $J \rightarrow J' \neq J$. Then for isotropic Raman Q lines the off-diagonal elements of the collision cross-section matrix are defined by Eq. (3)

$$\sigma_{J'J} \equiv \sigma_{J' \leftarrow J} = -\overline{v}^{-1} \int_0^{b_{\max}} 2\pi b db \left\langle v \cdot P_{J'J} \right\rangle_{v,O} \equiv -\overline{v}^{-1} \left\langle v \cdot P_{J'J} \right\rangle_{b,v,O}, \qquad \text{(A1)}$$

where $\overline{v} = \sqrt{\dfrac{8k_B T}{\pi\mu}}$ is mean relative speed of colliding pair, b_{max} is maximum value of the impact parameter; $P_{J'J}$ is the probability ("index") of $J \rightarrow J'$ transition in collision, namely,

$P_{J'J} = 1$ if in given collision the transition $J \to J'$ occurs (all others $P_{J''J}$ $(J'' \neq J')$ are set equal to zero).

The diagonal elements of the collision cross-section matrix σ_{JJ} are defined by Eq. (3) as follows

$$\sigma_{JJ} = \bar{v}^{-1} \int_0^{b_{\max}} 2\pi b db \left\langle v \cdot (1 - P_{JJ}) \right\rangle_{v,O} \equiv \bar{v}^{-1} \left\langle v \cdot (1 - P_{el}(J)) \right\rangle_{b,v,O}, \qquad \text{(A2)}$$

where $P_{JJ} \equiv P_{el}(J)$ is the probability ("index") that given collision starting from level J is elastic. The diagonal cross-section σ_{JJ} characterizes the total inelastic rate from J level. Note that the right-hand part of the Eq. (A2) is simply the pressure broadening cross-section of the half-width of isotropic Raman Q line.

Summing Eq. (A1) over $J' \neq J$ from 0 to J'_{max} (which must be high enough to include *all possible* inelastic transitions from J level), we arrive at:

$$\sum_{J' \neq J}^{J'_{\max}} \sigma_{J'J} = -\bar{v}^{-1} \left\langle v \sum_{J' \neq J}^{J'_{\max}} P_{J'J} \right\rangle_{b,v,O} = \\ = -\bar{v}^{-1} \left\langle v \cdot P_{inel}(J) \right\rangle_{b,v,O} = -\bar{v}^{-1} \left\langle v \cdot (1 - P_{el}(J)) \right\rangle_{b,v,O}, \qquad \text{(A3)}$$

since $\sum_{J' \neq J}^{J'_{\max}} P_{J'J} \equiv P_{inel}(J) \equiv 1 - P_{el}(J)$.

Comparing Eq. (A2) and Eq. (A3) we obtain

$$\sum_{J' \neq J}^{J'_{\max}} \sigma_{J'J} = -\sigma_{JJ}, \qquad \text{(A4)}$$

or, equivalently,

$$\sum_{J'=0}^{J'_{\max}} \sigma_{J'J} = 0. \qquad \text{(A5)}$$

The elements of the relaxation matrix $W = n\bar{v}\sigma$ are straightforward

$$W_{J'J} = n\bar{v}\sigma_{J'J}, \qquad W_{JJ} = n\bar{v}\sigma_{JJ} \qquad \text{(A6)}$$

They also obey the sum rule

$$\sum_{J' \neq J}^{J'_{\max}} W_{J'J} = -W_{JJ} \quad , \text{ or } \sum_{J'=0}^{J'_{\max}} W_{J'J} = 0 \quad . \tag{A7}$$

Note that sum rule Eq. (A4), Eq. (A5) or Eq. (A7) is exactly valid for both C3D and C3Diso classical methods for the Q lines of isotropic Raman scattering when vibrational phase shifts are neglected.

2. The Gordon-McGinnis symmetrization procedure[20] for re-establishing the detailed balance leads to a ***new expression*** for the off-diagonal elements:

$$\sigma^{DB}_{J'J} = \frac{1}{N_J + N_{J'}} \left\{ N_J \sigma_{J'J} + \frac{p_{J'}}{p_J} N_{J'} \sigma_{JJ'} \right\} \tag{A8}$$

Here N_J and $N_{J'}$ are the numbers of trajectories from which $\sigma_{J'J}$ and $\sigma_{JJ'}$ are computed respectively ($p_{J'}$ and p_J are defined in the main text). It is not surprising that these artificially changed values of the cross-sections $\sigma^{DB}_{J'J}$ no longer obey exactly the sum rule. In other words, artificially imposing detailed balance, Eq. (A8), spoils the sum rule. From our exact classical C3D calculations, it follows that the sum rule is satisfied only approximately, i.e., $W^{DB}_{JJ} \approx -\sum_{J' \neq J} W^{DB}_{J'J}$ (however, with fair accuracy as is seen from the Table IV).

References

[1]J.M. Hartmann, C. Boulet, and D. Robert, *Collisional Effects on Molecular Spectra, Laboratory Experiments and Models, Consequences for Applications* (Elsevier, Amsterdam, 2008).

[2]L.S. Rothman, N. Jacquinet-Husson, C. Boulet, and A.M. Perrin, Comptes Rendus – Physique **6**, 897 (2005).

[3]J.J. Harrison, P.F. Bernath, and G. Kirchengast, J. Quant. Spectrosc. Radiat. Transfer **112,** 2347 (2011).

[4]R. Shafer and R.G. Gordon, J. Chem. Phys. **58,** 5422 (1973).

[5]P. McGuire and D.J. Kouri, J. Chem. Phys. **60,** 2488 (1974).

[6]P.W. Anderson, Phys. Rev. **76**, 647 (1949).

[7]C.J. Tsao and B. Curnutte, J. Quant. Spectrosc. Radiat. Transfer **2**, 41 (1962).

[8]W.B. Neilsen and R.G. Gordon, J. Chem. Phys. **58,** 4131 (1973).

[9]W.B. Neilsen and R.G. Gordon, J. Chem. Phys. **58,** 4149 (1973).

[10]E.W. Smith, M. Giraud, and J. Cooper, J. Chem. Phys. **65**, 1256 (1976).

[11]D. Robert and J. Bonamy, J. Phys. (Paris) **10**, 923 (1979).

[12]R. Lynch, R.R. Gamache, and S.P. Neshyba, J. Chem. Phys. **105**, 5711 (1996).

[13]Q. Ma, C. Boulet, and R.H. Tipping, J. Chem. Phys. **139**, 034305 (2013).

[14]J. Buldyreva, N. Lavrentieva, and V. Starikov, *Collisional Line Broadening and Shifting of Atmospheric Gases: A Practical Guide for Line Shape Modeling by Current Semiclassical Approaches* (Imperial College Press; 2011).

[15]R.G. Gordon, J. Chem. Phys. **44**, 3083 (1966).

[16]R.G. Gordon, J. Chem. Phys. **45**, 1649 (1966).

[17]R.G. Gordon, J. Chem. Phys. **46**, 448 (1967).

[18]R.G. Gordon and R.P. McGinnis, J. Chem. Phys. **49**, 2455 (1968).

[19]R.G. Gordon, Adv. Magnetic Resonance **3**, 1 (1968).

[20]R.G. Gordon and R.P. McGinnis, J. Chem. Phys. **55**, 4898 (1971).

[21]S.V. Ivanov, Molec. Phys. **102**, 1871 (2004).

[22]S.V. Ivanov. Trajectory study of CO_2-Ar and CO_2-He collision complexes// In: *Weakly Interacting Molecular Pairs: Unconventional Absorbers of Radiation in the Atmosphere.* Ed. by Claude Camy-Peyret and Andrei A. Vigasin. NATO Science Series IV: Earth and Environmental Sciences. V. 27. Kluwer Academic Publishers, Boston/Dordrecht/London, 2003, P. 49-63.

[23]J.M. Hartmann and C. Boulet, J. Chem. Phys. **113**, 9000 (2000).

[24]C. Boulet, Q. Ma, and F. Thibault, J. Chem. Phys. **140**, 084310 (2014).

[25]S.V. Ivanov and O.G. Buzykin, Molec. Phys. **106**, 1291 (2008).

[26]F. Thibault, L. Gomez, S.V. Ivanov, O.G. Buzykin, and C. Boulet, J. Quant. Spectrosc. Radiat. Transfer **113**, 1887 (2012).

[27]S.V. Ivanov and O.G. Buzykin, J. Quant. Spectrosc. Radiat. Transfer **119**, 84 (2013).

[28]M.L. Koszykovski, R.L. Farrow, and R.E. Palmer, Opt. Lett. **10**, 478 (1985).

[29]F. Thibault, C. Boulet, and Q. Ma, J. Chem. Phys. **140**, 044303 (2014).

[30]L. Gomez, B. Bussery-Honvault, T. Cauchy, M. Bartolomei, D. Cappelletti, and F. Pirani, Chem. Phys. Lett. **445,** 99 (2007); D. Cappelletti, F. Pirani, B. Bussery-Honvault, L. Gomez, and M. Bartolomei, Phys. Chem. Chem. Phys. **10,** 4281 (2008).

[31]F. Thibault, R. Z. Martinez, D. Bermejo, and L. Gomez, J. Quant. Spectrosc. Radiat. Transfer **112**, 2542 (2011).

[32]C.W. Gear, *Numerical Initial Value Problems in Ordinary Differential Equations* (Englewood Cliffs: Prentice-Hall, N.J., 1971).

[33]R.E. Langer, Phys Rev. **51**, 669 (1937).

[34]S. Chapman and S. Green, J. Chem. Phys. **67**, 2317 (1977).

[35]G.O. Sitz and R.L. Farrow, J. Chem. Phys. **93**, 7883 (1990).

[36]G.J. Rosasco, W. Lempert, and W.S. Hurst, Chem. Phys. Lett. **97**, 435 (1983).

[37]B. Lavorel, G. Millot, R. Saint-Loup, C. Wenger, H. Berger, J.P. Sala, J. Bonamy, and D. Robert, J. Phys. (Paris) **47**, 417 (1986).

TABLE I. One body rate constants for $J \rightarrow J'$ transitions in N_2 at 298 K in $\mu s^{-1}Torr^{-1}$. Comparison of classical C3D and C3Diso results with fully quantum CC/CS results from Ref. 29 and with the experimental data of Sitz and Farrow.[35] The first (upper) figures in each cell for classical C3D and C3Diso columns correspond to results with imposed detailed balance applied via the symmetrizing procedure of Gordon and McGinnis (see text), the second (lower) ones – to raw trajectory results (no imposed detailed balance).

J	*J'*	Experiment	Quantum CC/CS	Classical C3D	Classical C3Diso
0	2	6.64±1.18	7.23	7.46	7.64
				7.98	7.46
0	4	3.76±0.83	3.78	4.20	3.34
				4.95	3.36
0	6	2.73±0.61	2.58	2.64	1.91
				3.03	1.95
0	8	0.86±0.51	1.69	1.73	1.42
				1.80	1.45
0	10	0.64±0.12	0.94	0.98	0.95
				0.93	0.98
0	12	0.29±0.06	0.45	0.46	0.61
				0.36	0.63
0	14	0.22±0.04	0.175	0.19	0.35
				0.13	0.36
2	4	5.13±0.58	4.52	5.09	4.51
				5.83	4.66
2	6	2.40±0.44	2.83	2.97	2.04
				3.35	2.20
2	8	1.52±0.34	1.81	1.85	1.32
				1.97	0.99
2	10	0.97±0.22	1.01	1.03	0.87
				0.97	1.47
2	12	0.28±0.14	0.49	0.49	0.53
				0.42	0.61
2	14	0.12±0.04	0.19	0.22	0.32
				0.15	0.38
4	6	4.7±0.6	3.74	4.08	3.58
				4.53	3.83
4	8	2.2±0.4	2.12	2.24	1.60
				2.36	1.81
4	10	1.4±0.2	1.15	1.22	0.94
				1.16	1.14
4	12	0.54±0.13	0.56	0.62	0.56
				0.53	0.70
4	14	0.21±0.04	0.22	0.25	0.31
				0.19	0.41
6	8	3.37±0.47	3.18	3.33	3.06
				3.69	3.35
6	10	2.22±0.29	1.51	1.57	1.33
				1.59	1.58
6	12	0.71±0.14	0.77	0.74	0.71

				0.67	0.92
6	14	0.23±0.05	0.28	0.32	0.36
				0.27	0.50
8	10	2.52±0.41	2.65	2.88	2.70
				3.09	2.98
8	12	1.12±0.22	1.07	1.19	1.08
				1.20	1.36
8	14	0.29±0.07	0.39	0.50	0.50
				0.42	0.69
10	12	2.68±0.43	2.26	2.46	2.41
				2.66	2.74
10	14	1.04±0.13	0.72	0.89	0.86
				0.91	1.11
12	14	1.83±0.26	1.96	2.13	2.16
				2.32	2.52

TABLE II. Relaxation matrix W for N_2-N_2 at 298 K. The $W_{J'J}$ elements are expressed in 10^{-3} $cm^{-1}atm^{-1}$. Each cell contains five positions corresponding to the results obtained using different methods: 1-st - quantum CC/CS from Ref. 29; 2-nd - exact C3D with imposed detailed balance; 3-rd - exact C3D raw data (no imposed detailed balance); 4-th - C3Diso with imposed detailed balance; 5-th C3Diso raw data (no imposed detailed balance).

J J'	0	2	4	6	8	10	12	14
0	68.2	-6.2	-2.1	-1.22	-0.82	-0.54	-0.34	-0.19
	70.06	-6.38	-2.28	-1.23	-0.82	-0.54	-0.33	-0.20
	70.06	-7.31	-2.56	-1.36	-0.92	-0.55	-0.34	-0.21
	67.07	-6.53	-1.80	-0.80	-0.67	-0.53	-0.44	-0.37
	67.07	-7.18	-1.72	-0.67	-0.44	-0.24	-0.15	-0.089
2	-29.2	50.3	-11.6	-6.3	-4.1	-2.7	-1.69	-0.97
	-30.11	55.04	-13.04	-6.51	-4.15	-2.68	-1.68	-1.11
	-29.04	55.04	-12.72	-6.68	-4.16	-2.59	-1.66	-1.12
	-30.84	50.64	-11.57	-4.47	-2.97	-2.27	-1.80	-1.59
	-30.10	50.64	-10.93	-3.54	-1.93	-1.05	-0.65	-0.38
4	-15.3	-18.3	46.0	-13.0	-7.53	-4.8	-3.05	-1.75
	-16.95	-20.52	49.83	-14.08	-7.87	-5.03	-3.36	-1.91
	-16.65	-20.83	49.83	-14.03	-7.91	-4.98	-3.34	-1.88
	-13.47	-18.21	46.37	-12.35	-5.62	-3.87	-3.03	-2.43
	-13.56	-18.79	46.37	-11.10	-4.30	-2.15	-1.32	-0.71
6	-10.46	-11.5	-15.1	44.4	-13.14	-7.3	-4.9	-2.575
	-10.66	-11.98	-16.45	47.34	-13.72	-7.54	-4.64	-2.94
	-10.51	-11.8	-16.50	47.34	-13.40	-7.48	-4.64	-2.92
	-7.71	-8.22	-14.43	43.24	-12.58	-6.37	-4.46	-3.29
	-7.87	-8.89	-15.47	43.24	-11.11	-4.63	-2.39	-1.21
8	-6.84	-7.33	-8.6	-12.9	44.0	-12.57	-6.67	-3.59
	-6.98	-7.48	-9.02	-13.45	46.09	-13.57	-7.32	-4.42
	-6.87	-7.47	-8.98	-13.77	46.09	-13.42	-7.29	-4.48
	-5.73	-5.35	-6.44	-12.33	40.91	-12.72	-6.67	-4.44
	-5.87	-5.94	-7.29	-13.51	40.91	-11.27	-4.58	-2.31
10	-3.81	-4.1	-4.67	-6.12	-10.73	42.3	-11.8	-5.5
	-3.95	-4.14	-4.94	-6.33	-11.63	44.71	-12.99	-6.81
	-3.95	-4.22	-4.99	-6.39	-11.78	44.71	-12.80	-6.67
	-3.85	-3.51	-3.80	-5.35	-10.90	39.16	-12.72	-6.59
	-3.96	-3.98	-4.60	-6.37	-12.03	39.16	-10.95	-4.68
12	-1.84	-1.97	-2.26	-3.13	-4.34	-9.13	40.1	-11.37
	-1.86	-1.99	-2.52	-2.98	-4.80	-9.93	42.97	-12.46
	-1.84	-2.01	-2.54	-2.98	-4.83	-10.11	42.97	-12.17
	-2.47	-2.13	-2.28	-2.87	-4.37	-9.73	37.04	-12.61
	-2.56	-2.48	-2.84	-3.70	-5.49	-11.05	37.04	-10.53
14	-0.7	-0.77	-0.88	-1.13	-1.6	-2.9	-7.92	34.1
	-0.78	-0.90	-0.99	-1.31	-2.00	-3.59	-8.60	40.30
	-0.78	-0.89	-1.02	-1.33	-1.94	-3.72	-8.88	40.30
	-1.41	-1.30	-1.26	-1.46	-2.01	-3.48	-8.70	34.27
	-1.47	-1.53	-1.64	-2.02	-2.78	-4.49	-10.17	34.27

TABLE III. Relative errors $\sum_{J'=0}^{28} (W_{J'J}^{NDB} - W_{J'J}^{DB}) / W_{J'J}^{DB}$ (in %) in the detailed balance in the raw classical calculations of relaxation matrix elements $W_{J'J}$: C3D (upper value) and C3Diso (lower value). DB – modified results with final application of detailed balance symmetrization by Eq. (5), NDB – raw, unsymmetrized results, i.e., no imposed detailed balance by Eq. (5).

J ***J'***	**0**	**2**	**4**	**6**	**8**	**10**	**12**	**14**
0	0	14.6	12.1	10.7	12.1	1.1	3.3	3.6
	0	9.9	-5.3	-24.6	-35.3	-53.8	-65.4	-75.8
2	-3.6	0	-2.5	2.6	0.2	-3.2	-1.3	1.1
	-2.4	0	-5.6	-20.7	-35.0	-53.7	-64.0	-76.1
4	-1.8	1.5	0	-0.3	0.5	-1.0	-0.6	-1.4
	0.7	3.2	0	-10.1	-23.4	-44.5	-56.6	-70.7
6	-1.3	-1.4	0.3	0	-2.4	-0.8	-0.1	-0.9
	2.0	8.1	7.2	0	-11.7	-27.3	-46.4	-63.2
8	-1.6	-0.1	-0.4	2.4	0	-1.1	-0.38	1.3
	2.4	11.1	13.2	9.6	0	-11.4	-31.2	-47.9
10	-0.2	2.0	1.0	1.0	1.3	0	-1.4	-1.9
	3.0	13.4	21.0	19.1	10.4	0	-13.9	-29.0
12	-0.6	1.0	0.8	0.1	0.6	1.8	0	-2.3
	3.7	16.5	24.5	29.1	25.6	13.6	0	-16.5
14	-1.0	-1.4	2.7	2.0	-3.1	3.6	3.2	0
	4.2	17.8	30.4	38.3	38.7	29.0	16.9	0

TABLE IV. The relative error $|\sum_{J'=0}^{28} W_{J'J}|/W_{JJ}$ (in %) of the sum rule $\sum_{J'=0}^{28} W_{J'J} = 0$ in classical calculations. DB – modified results with final application of detailed balance symmetrization by Eq. (5), NDB – raw, unsymmetrized results, i.e., no imposed detailed balance.

J	C3D, DB	C3D, NDB	C3Diso, DB	C3Diso, NDB
0	2.39	$1.13\cdot10^{-2}$	$8.2\cdot10^{-3}$	$1.35\cdot10^{-2}$
2	0.90	$1.52\cdot10^{-2}$	7.7	$4.5\cdot10^{-2}$
4	0.90	$1.69\cdot10^{-2}$	15.7	$7.24\cdot10^{-2}$
6	0.47	$1.78\cdot10^{-2}$	21.47	$9.85\cdot10^{-2}$
8	0.45	$1.84\cdot10^{-2}$	22.84	0.15
10	0.26	$1.9\cdot10^{-2}$	17.75	0.19
12	0.73	$2.0\cdot10^{-2}$	4.6	0.27
14	0.82	$2.1\cdot10^{-2}$	18.0	0.38

Figure captions

FIG. 1. Relative errors of C3D (a) and C3Diso (b) results presented in Table I versus quantum CC/CS data. DB – detailed balance.

FIG. 2. Comparison between calculated half-widths (diagonal elements of *W* matrix) for N_2-N_2 Raman Q lines at $T = 298$ K. Theory: *1* – semi-classical refined Robert-Bonamy formalism,[13, 24] *2* – quantum CC/CS results,[26] *3* – present exact classical C3D method, *4* - present classical C3Diso method. Experimental data: *5* – Ref. 31 , *6* – Ref. 36, *7* – Ref. 37.

FIG. 3. Comparison of the present classical calculations with the quantum CC/CS results of Ref. 36 and refined semi-classical RB data of Ref. 24 for selected off-diagonal elements at $T = 298$ K. $J = 4$ (a), $J = 6$ (b), $J = 8$ (c).

1 – semi-classical refined RB formalism (see Fig. 1 of Ref. 24); *2* – quantum CC/CS results of Ref. 36; *3* – present classical C3D method with imposed detailed balance; *4* – C3D raw data; *5* – present classical C3Diso method with imposed detailed balance; *6* – C3Diso raw data; 7 – corrected semi-classical refined RB formalism (see Fig. 3 of Ref. 24).

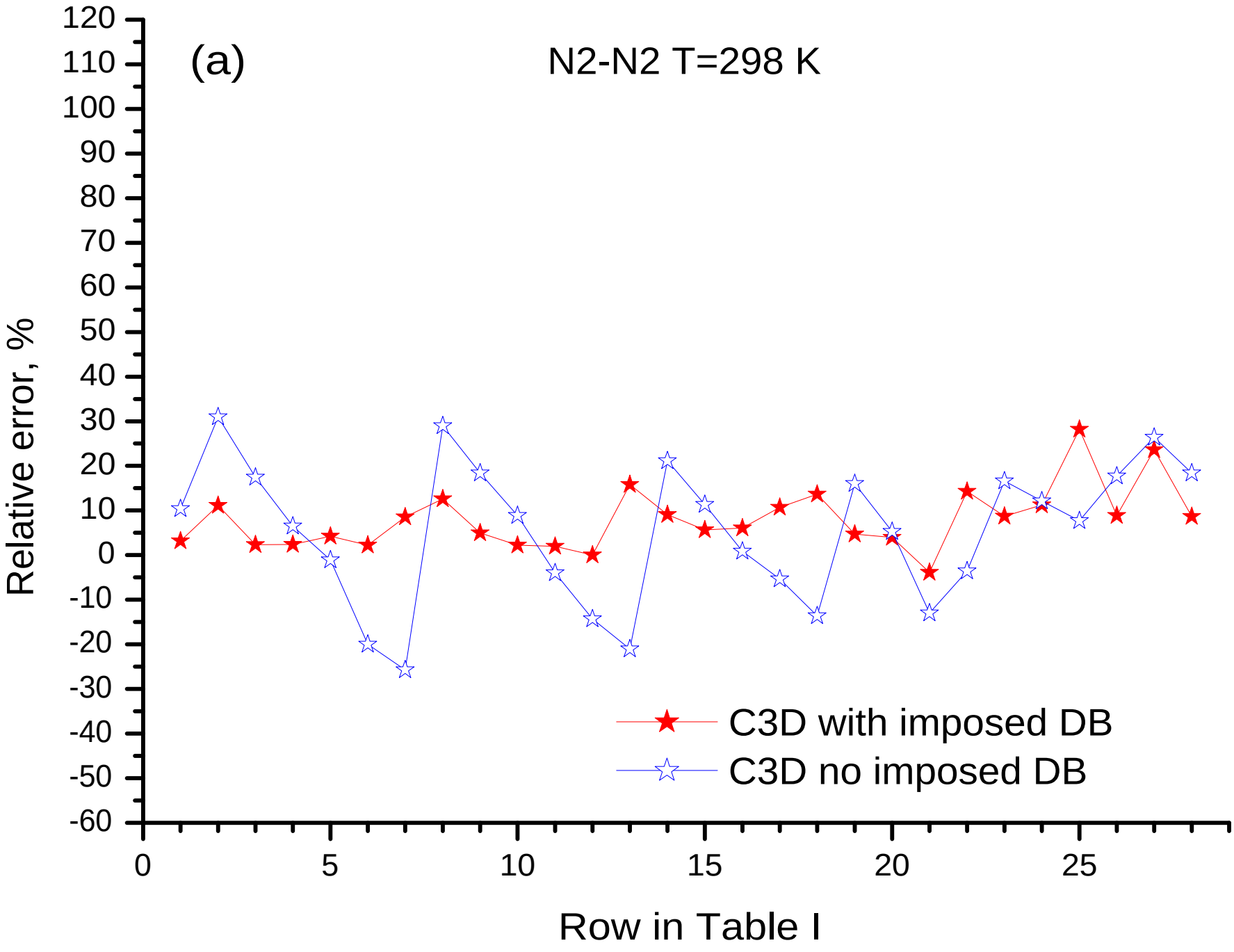
(a)
N2-N2 T=298 K
Relative error, %
120
110
100
90
80
70
60
50
40
30
20
10
0
-10
-20
-30
-40
-50
-60
0
5
10
15
20
25
Row in Table I
C3D with imposed DB
C3D no imposed DB

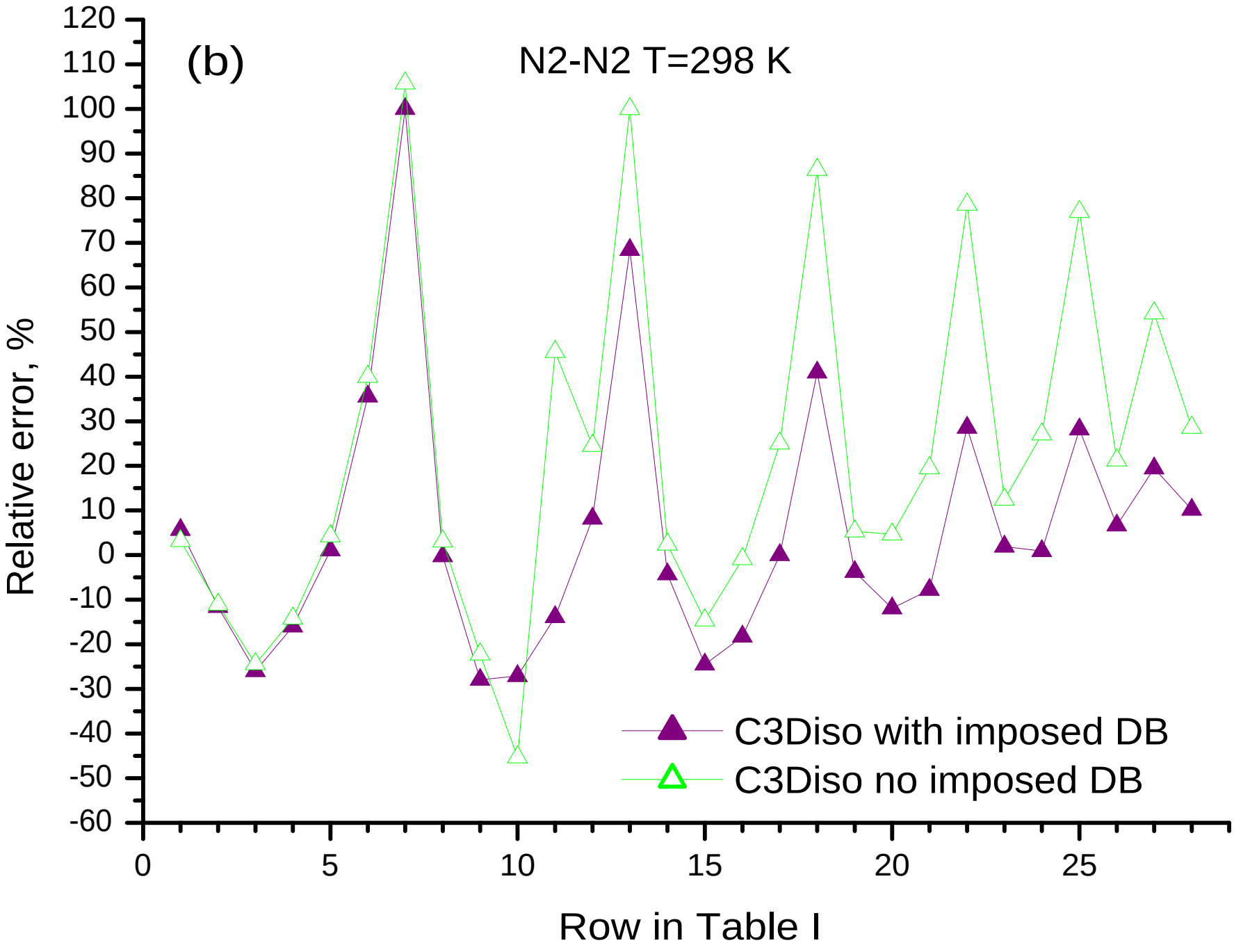
(b)
N2-N2 T=298 K
Relative error, %
Row in Table I
C3Diso with imposed DB
C3Diso no imposed DB
120
110
100
90
80
70
60
50
40
30
20
10
0
-10
-20
-30
-40
-50
-60
0
5
10
15
20
25

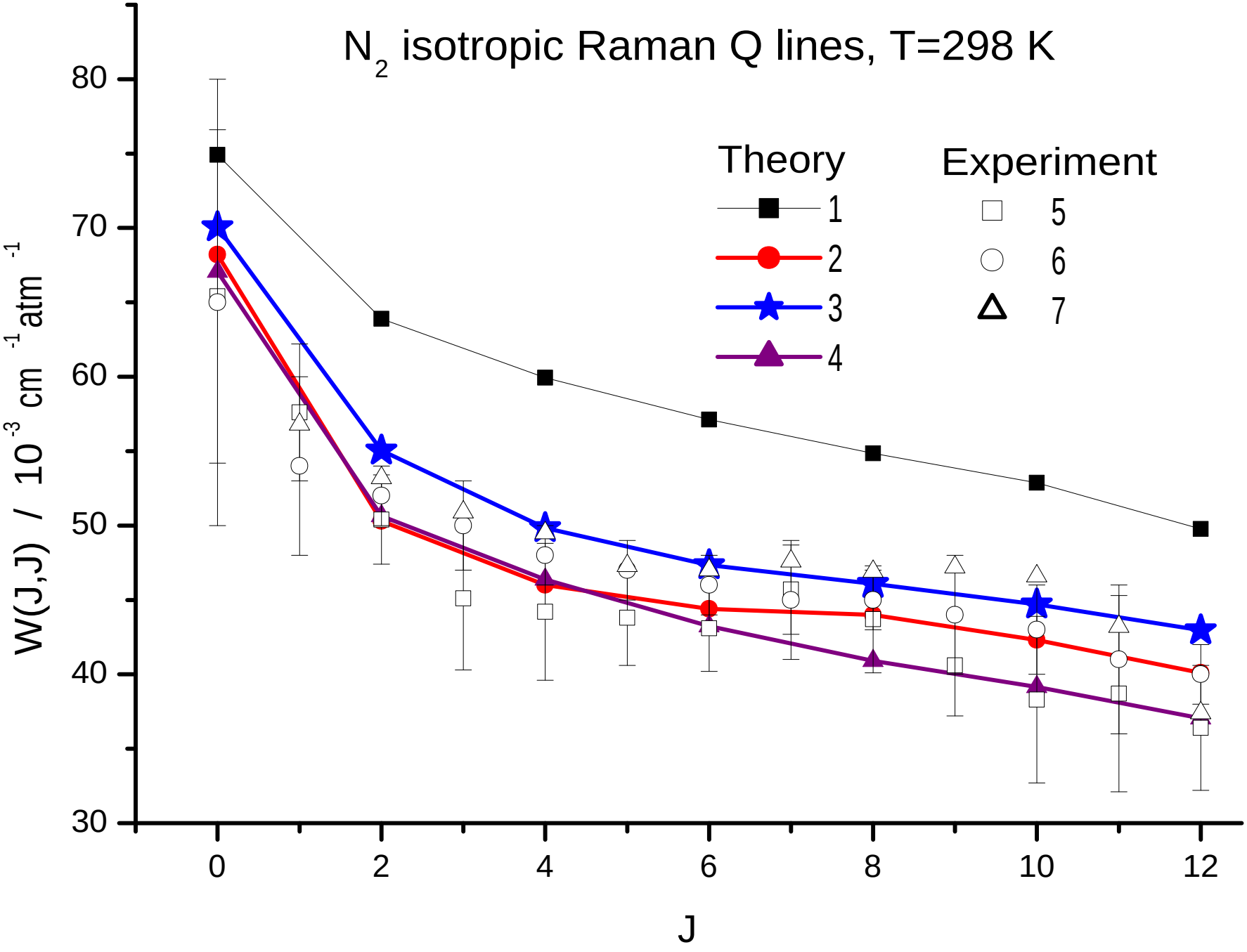
N2 isotropic Raman Q lines, T=298 K
Theory
1
2
3
4
Experiment
5
6
7
W(J,J) / 10-3 cm-1atm-1
80
70
60
50
40
30
0
2
4
6
8
10
12
J

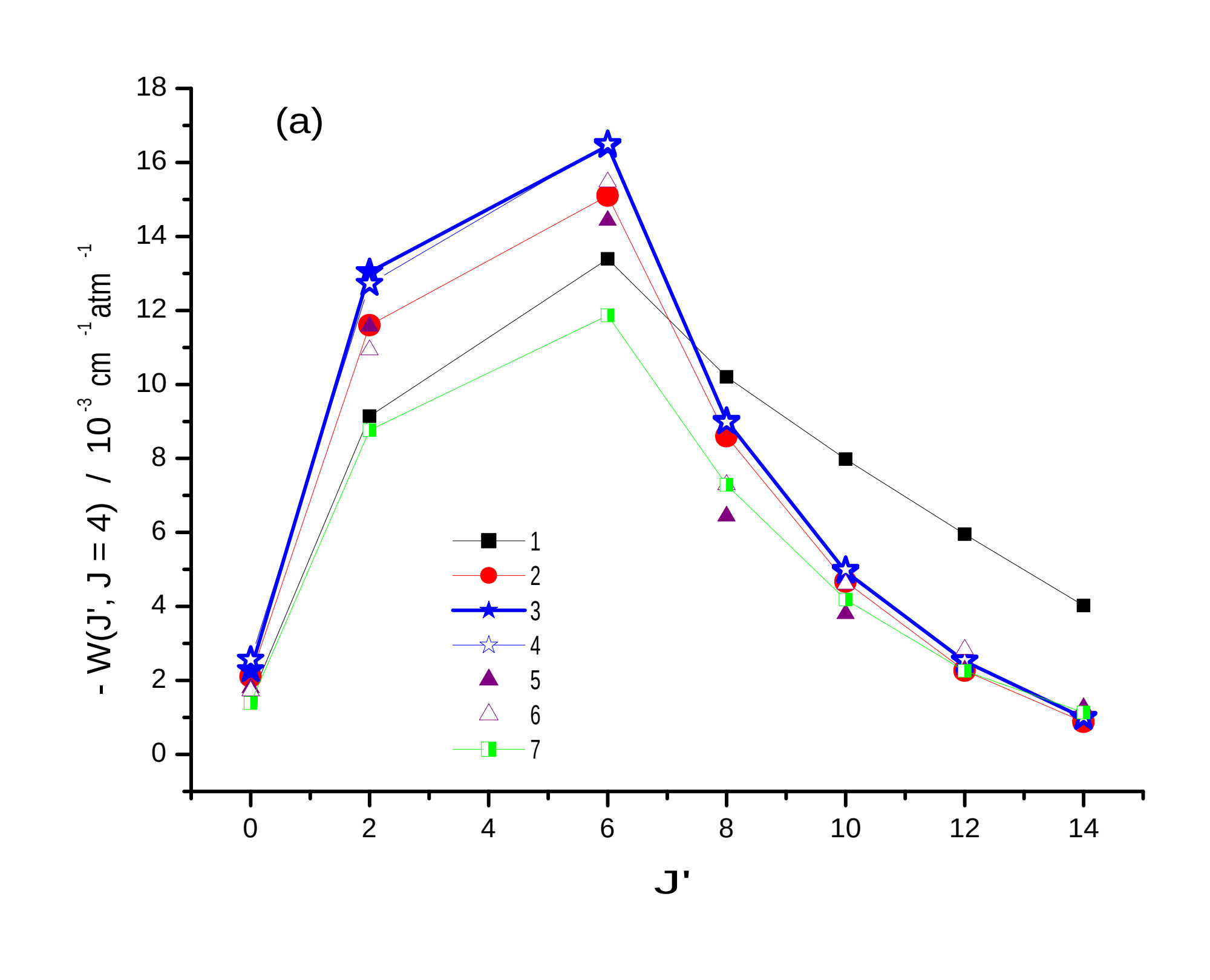
(a)
- W(J', J = 4) / 10^-3 cm^-1 atm^-1
J'
0
2
4
6
8
10
12
14
16
18
1
2
3
4
5
6
7

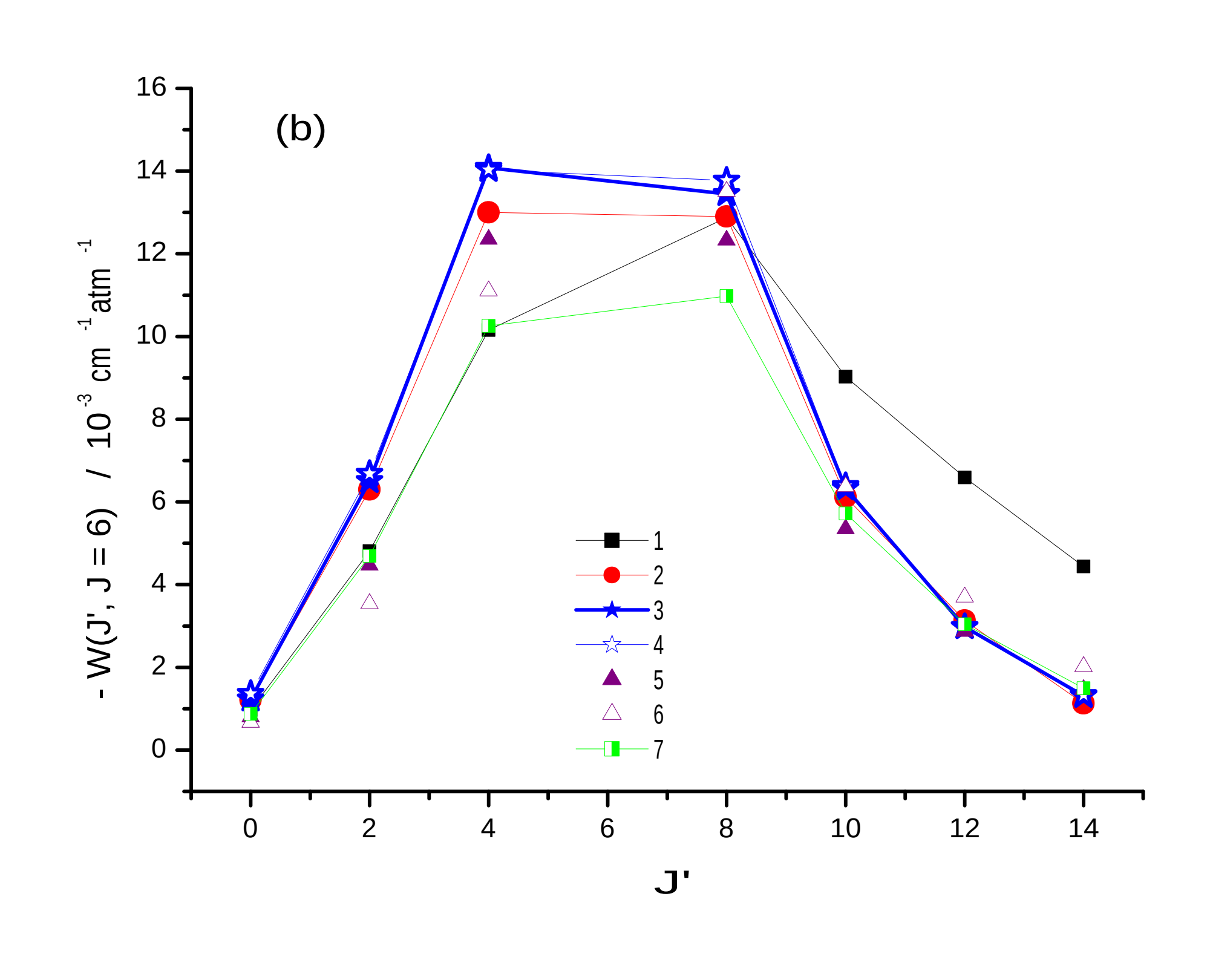
(b)
- W(J', J = 6) / 10^-3 cm^-1 atm^-1
J'
0
2
4
6
8
10
12
14
16
1
2
3
4
5
6
7

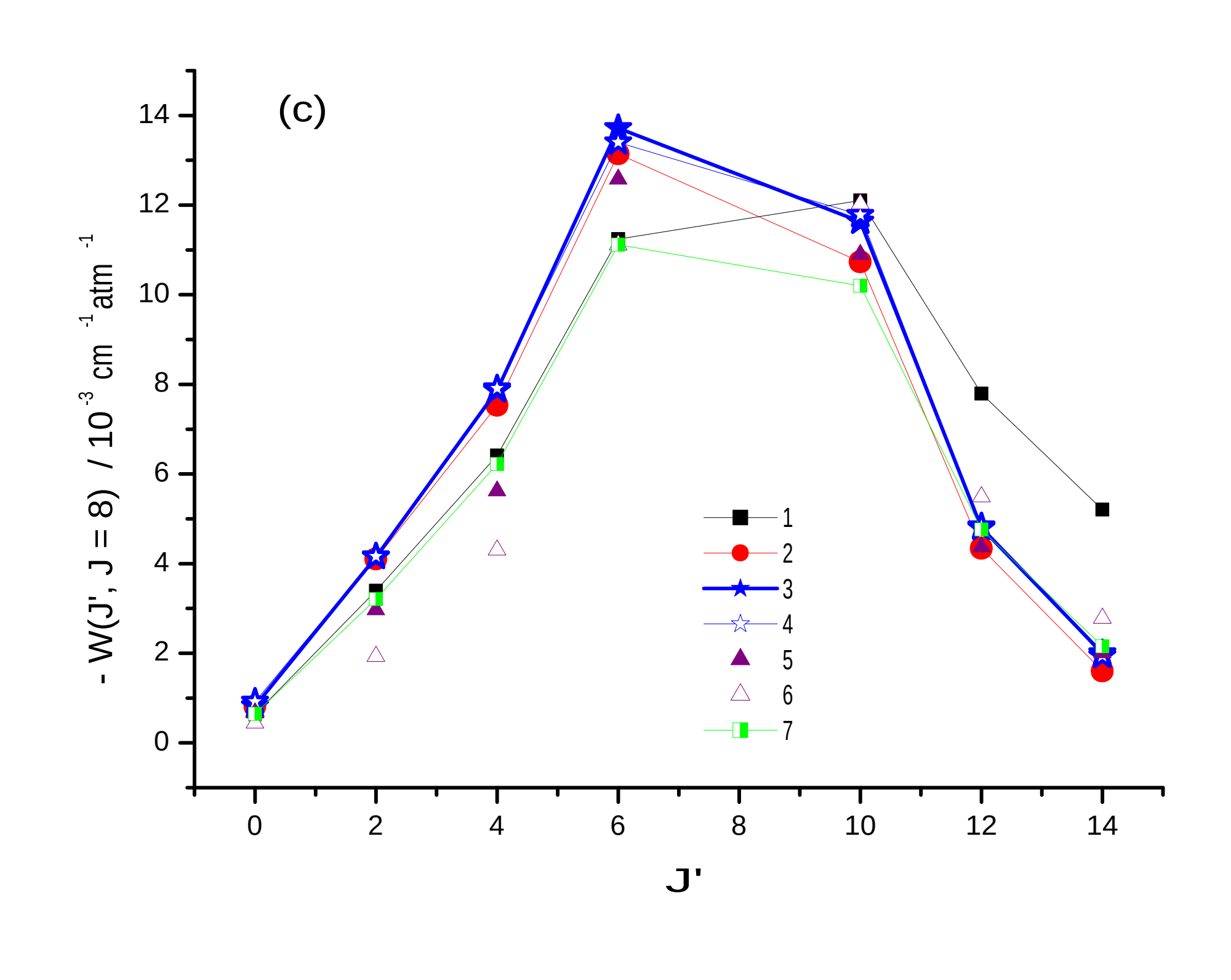
(c)
- W(J', J = 8) / 10^-3 cm^-1 atm^-1
J'
0
2
4
6
8
10
12
14
1
2
3
4
5
6
7